Finite Element Modeling Of Deformation Load in Al1200 Deep Drawing

Oluwole.O.O and Falana.O.K

Abstract--In industry, deformation load is usually the interest of a production engineer when it comes to the production of deep drawn products. In this work Finite Element Method has been employed to predict the deformation load in the production of 9"˚ holloware taking advantage of the mechanical action of the punch and the die.

The chosen geometry was the axial section of a 228.6/100 (Dia/height) holloware. The geometry was drawn on the Graphic User Interface of COMSOL MULTIPHYSICS and mechanical properties of aluminium A1200, such as the Young's modulus of elasticity (69GPa), Poisson's ratio (0.3), density (2590Kgm^{-3}) and yield stress (130MPa) were applied to the geometry. The choice of elasto-plasticity was applied. Geometric non-linearities present in the problem were also accounted for. A prescribed punch velocity of 65mms^{-1} was imposed as the boundary condition. The whole domain of the geometry was finely meshed, a Von Mises yield surface was considered and the model studied on the Graphic User Interface.

The results showed that a maximum deformation force (*125KN*) was obtained at the inner fillet region of the pot. The values of Von-Mises /effective stress (*1.603 x 10^{5}Nm^{-2}*), stress tensor (*1.429 x 10^{5}Nm^{-2}*), strain tensor (*1.91 x 10^{-6}*) and first Piola – Kirchhoff's stress (*1.429 x 10^{5}Nm^{-2}*) were obtained.

Result from industry showed agreement with the results obtained using the finite element modeling.

Index Terms--*deformation load, deep drawing, hollowware, elastic-plastic deformation, finite element method*

1 INTRODUCTION

The shape of many metal products, which are used in daily life, is obtained by means of Sheet Metal Forming (SMF) processes. Generally, SMF processes are characterized by permanent deformation of a metal sheet. This permanent or plastic deformation is attained by the application of an external load on the sheet. This load must be sufficiently high to ensure that after removing the load the specific shape of the sheet is retained. Obtaining such a sufficiently high load for permanent deformation of metal sheet

requires a complete, accurate and detailed knowledge of the process. Sheet metal forming operation involves complex physical mechanisms that give rise to a high order non-linear problem. Apart from the nonlinearity induced by the contact and the friction, there is a geometrical non-linearity caused by large displacement and large deformation. Furthermore, non-linear material behaviors such as plasticity make the problem even more difficult to be solved analytically.

Deep drawing is a metal forming process in which sheet metal is stretched into the desired part shape. A tool pushes downward on the sheet metal, forcing it into a die cavity in the shape of the desired part. The tensile forces applied to the sheet cause it to plastically deform into a cup-shaped part. Deep drawn parts are characterized by a depth equal to more than half of the diameter of the part. These parts can have a variety of cross sections with straight, tapered, or even curved walls, but cylindrical or rectangular parts are most common. Deep drawing is most effective with ductile metals, such as aluminum, brass, copper, and mild steel. Examples of parts formed with deep drawing include automotive bodies and fuel tanks, cans, cups, kitchen sinks, and pots and pans.

The work of Sachs laid the foundation for the subsequent theoretical treatment for deep drawing[1]. Hill, studying the radial drawing problem considered the limiting cases of plane stress and strain [2]. A comprehensive study of the elementary mechanics of the drawing process was carried out and the model for bending over the die profile improved [3].It was noticed, however, that the solutions of these works were not extended to the punch nose region [4]. Numerical methods were further applied to analyse the radial drawing problem of anisotropic nature[5].

- *Dr. Oluleke O. Oluwole is a Senior Lecturer in the Mechanical engineering department of the University of Ibadan, Nigeria. E-mail: oluwoleo2@asme.org*
- *Falana is currently pursuing MSc degree program in Mechanical engineering in University of Ibadan, Nigeria. E-mail: falanamusic@yahoo.com*

According to Korhonen[4], the maximum drawing force at the limiting drawing ratio can be obtained by maximizing the drawing force at the beginning of the punch nose rounding with respect to the effective stress. This method assumes that there is no contact between the sheet and the punch at the point of necking (and fracture). Consequently, the frictional forces cannot assist in carrying the drawing load.

This force can be slightly higher (about 1.15 times the value just mentioned) due to the plane strain condition at the cup wall[6]. It has also been observed that, the higher the diameter of punch, the higher the punch force [7].

As observed by Siegert [8], during the deep drawing process, the drawing force increases from zero up to a maximum value and then falls down again to zero. The base is first formed in a manner similar to the stretch forming process and then the actual drawing process follows.

2 METHODOLOGY

The finite element method was applied in the determination of deformation load for Al 1200 deep drawing. The material used (Al 1200) , its chemical composition and properties are presented in Tables 1 and 2. Deformation geometry simulated was obtained from industry (Table 3) in order to be able to validate the modeled values with industry values. The model was drawn using COMSOL® multiphysics softwareand meshed(Fig.1). Perfectly plastic model was applied with the governing equations as expressed in section 2.3 to material deformation.Boundary values were applied as shown in Fig. 2.The relevant material mechanical properties in Table 1 were also applied to the model. The results were validated with values from industry.

TABLE 1
MECHANICAL PROPERTIES OF AL 1200

Property	Experimental value
Density	2.59×10^3 kgm^{-3}
Yield stress level	130MPa
Modulus of Elasticity	69GPa
Poisson ratio	0.3

TABLE 2
CHEMICAL COMPOSITION BY MASS OF AL 1200

Constituent element	Chemical compositions by mass (%)
Si + Fe	1.0
Cu	0.05
Mn	0.05
Zn	0.10
Ti	0.05
Others each	0.05
Others total	0.15
Aluminium	99.00

2.1 FE Modeling Assumptions

The following assumptions were made:
(1) Elastic strains are neglected, compared with plastic strains.
(2) The material is isotropic with non-linear strain-hardening.

(3) Radial, circumferential, and thickness directions are principal directions.
(4) Bending/unbending effects neglected for die profile radius to sheet thickness ratio greater than 6
(5) Shear stress is neglected across the thickness.
(6) The cup wall is straight [9]

2.2 Deformation Geometry

The industry dimension, deformation load and punch dimensions for the simulated deep –drawn hollowware as obtained from industry are presented in Table 3.

TABLE 3
DIMENSIONS OF HOLLOWWARE OBTAINED FROM INDUSTRY

Holloware Dia/Height. size (mm)	Def. load (KN)	Blank Dia/thickness (mm)	Die size (mm)		Punch size (mm)	
			Dia.	Height	Dia.	Height
228.6/100	120-150	390/4.3	450	100	220	200

2.3 Model Governing Equations

1. Von Mises (or effective stress) yield surface is applicable

$$\bar{\sigma} = \sqrt{\frac{1}{2}[(\sigma_r - \sigma_\theta)^2 + (\sigma_\theta - \sigma_t)^2 + (\sigma_t - \sigma_r)^2]} \quad (1)$$

2. Plastic incremental strains for the three principal directions: circumferential, thickness, and radial directions are expressed as:

$$\varepsilon_\theta = \ln\left(\frac{r}{R}\right) \quad (2a)$$

$$\varepsilon_t = \ln\left(\frac{t}{t_\theta}\right) \quad (2b)$$

$$\varepsilon_r = -\varepsilon_\theta - \varepsilon_t \quad (2c)$$

3. Effective incremental strain is described as:

$$d\bar{\varepsilon} = \sqrt{\frac{4}{3}\left[\left(d\varepsilon_\theta + d\varepsilon_t\right)^2 - d\varepsilon_\theta d\varepsilon_t\right]}. \quad (3)$$

4. The stress-strain relationship is based on Levy-Lode stress-strain equations.

$$\sigma_\theta - \sigma_r = \frac{2}{3}\frac{\bar{\sigma}}{d\bar{\varepsilon}}(d\varepsilon_\theta - d\varepsilon_r) = \frac{2}{3}\frac{\bar{\sigma}}{d\bar{\varepsilon}}(2d\varepsilon_\theta + d\varepsilon_t) \quad (4)$$

$$\sigma_t - \sigma_r = \frac{2}{3}\frac{\bar{\sigma}}{d\bar{\varepsilon}}(d\varepsilon_t - d\varepsilon_r) = \frac{2}{3}\frac{\bar{\sigma}}{d\bar{\varepsilon}}(2d\varepsilon_t + d\varepsilon_\theta) \quad (5)$$

5. The flow equation for strain hardening follows Ludwik-Hollomon power law:

$$\bar{\sigma} = C\bar{\varepsilon}^n \quad (6)$$

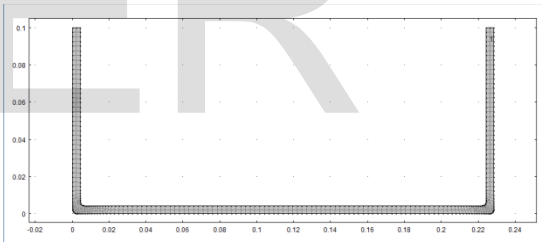

Fig. 1. Section through the wall with the mesh pattern

2.4 Boundary Conditions

The boundaries are shown in Fig. 2. The whole domain was divided into twelve and appropriate boundary conditions imposed.

Boundaries 5, 10 and 11 constrained to move with the punch velocity of 65mms^{-1} as shown in Fig. 3. The remaining boundaries were free to move relative to the velocity of the punch as shown in Fig. 4.

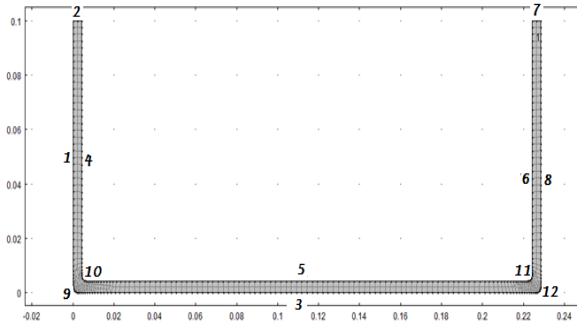

Fig. 2. Division of the domain into boundaries.

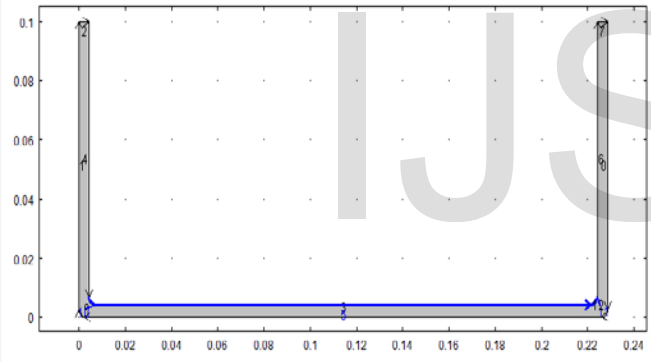

Fig. 3. Boundaries moving at 65mms^{-1}

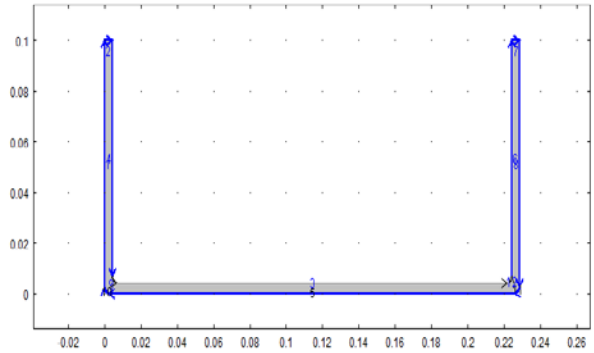

Fig. 4. Boundaries moving freely relative to thevelocity of the punch

3.0 Results

Figure 5 gives the effective stress distribution in the deep-drawn hollowware. It shows a maximum stress of 1.603 x 10^5Nm^{-2} .

Figure 6 shows an enlarged view of a corner of the hollowware where the maximum stress is experienced.

Figure 7 shows the plot of effective stress across the hollowware thickness at a punch travel of 50mm down the hollowware. It can be observed that the effective stress is minimum at the center of the wall thickness and maximum on both sides.

Figure 8 shows the plot of effective stresses down the hollowware wall at 2mm from the outside wall of the hollowware . It can be observed that the stress at the top of the hollowware is minimum increasing as the punch travels downwards. It can be observed as well that the stress value at the center of the wall thickness and punch travel of 50mm has the same value as in Figure 7 (4405.4723Nm^{-2}). The trends observed in Figures 7 and 8 can be seen to correspond with the distribution shown in Figure 6.

Figure 9 shows the effective stress Lode angle distribution in the deep-drawn hollowware.

Figure 10 shows the First Piola-Kirchoff stress distribution in the deep-drawing of the hollowware with a maximum of 1.429 x 10^5Nm^{-2}

Figure 11 shows the y component distribution of the stresstensor within the deep-drawn hollowarewith a maximum of 1.429 x 10^5Nm^{-2}.

Figure 12 shows the y component distribution of the strain tensorwithin the deep-drawn hollowarewith a maximum of 1.91 x 10^{-6}.

Table 2 shows the effective stress variation across the hollowware wall at a punch travel of 50mm. This is also presented graphically in Figure 7. The stress is observed to be least at the center of the wall thickness.

Table 3 shows the values of effective stress down the hollowware wall at distance 2mm from side wall. This is presented graphically in Figure 8. The stress is observed to be highest at the base of the deep-drawn hollowware and least at the top.

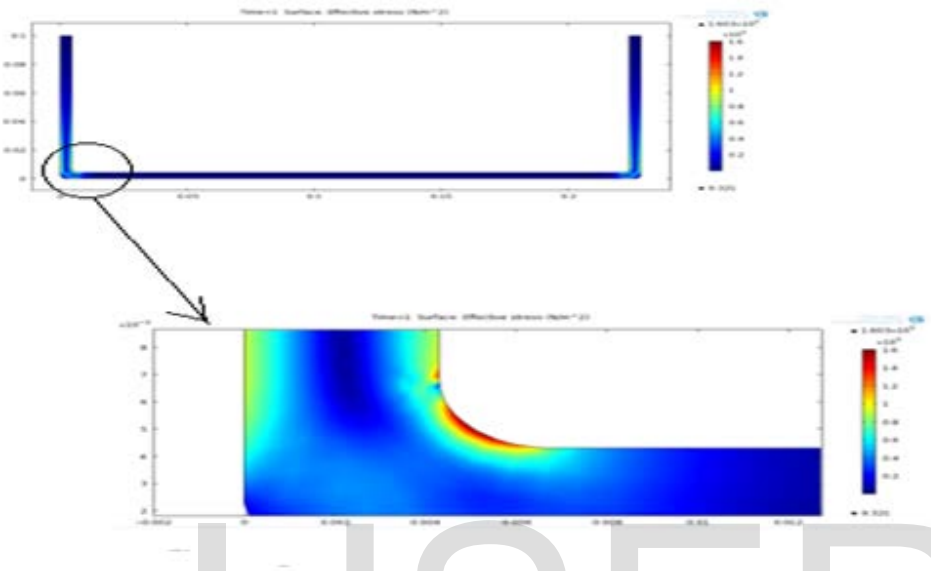

Fig. 5. Showing Effective stress and Fig.6. showing the region of maximum effective stress

TABLE 2
EFFECTIVE STRESS VARIATION ACROSS THE HOLLOWWARE WALL AT PUNCH TRAVEL OF 50MM

x – coordinate (m)	y – coordinate (m)	Effective stress (Nm^{-2})
1.28E-06	0.05	34982.8863
4.95E-04	0.05	26950.5231
9.98E-04	0.05	18820.9099
0.0015	0.05	10666.4682
0.002	0.05	4405.4723
0.0025	0.05	6853.4939
0.003	0.05	13932.7445
0.0035	0.05	21858.7613
0.004	0.05	29991.7556
0.0043	0.05	34410.4618

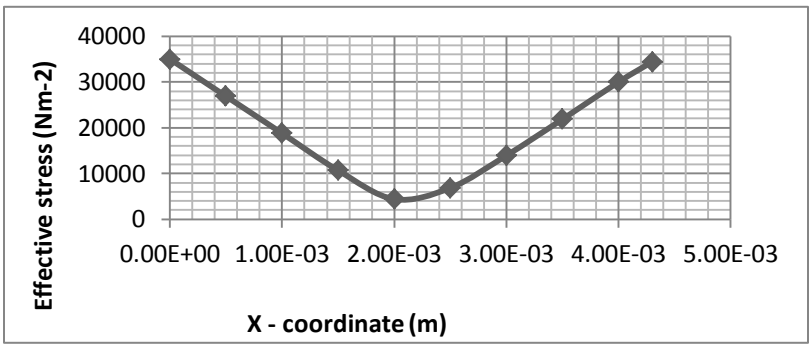

Fig. 7. Effective stress variation across hollowware thickness at punch travel of 50mm

TABLE 3
VALUES OF EFFECTIVE STRESS DOWN THE HOLLOWWARE WALL AT DISTANCE 2MM FROM OUTSIDE WALL.

X – coordinate (m)	Y - coordinate (m)	Effective Stress (Nm^{-2})
0.002	0.1	23.356
0.002	0.09	771.2354
0.002	0.08	1596.178
0.002	0.07	2526.275
0.002	0.06	3437.885
0.002	0.05	4413.893
0.002	0.04	5551.726
0.002	0.03	6386.202
0.002	0.02	7613.746
0.002	0.01	7871.388
0.002	0.005	27268.18
0.002	0.001	29490.08

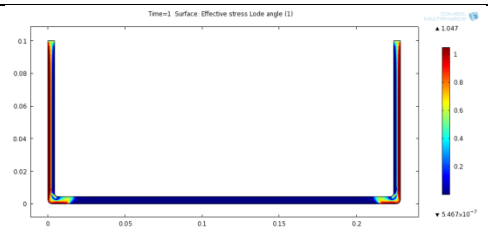

Fig. 9: Effective Stress Lode angle

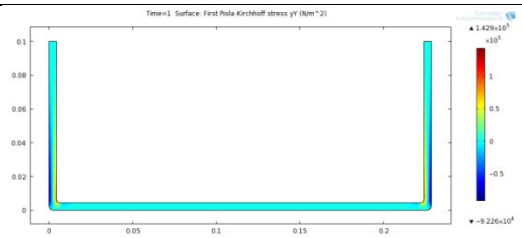

Fig. 10: First Piola-Kirchhoff Stress

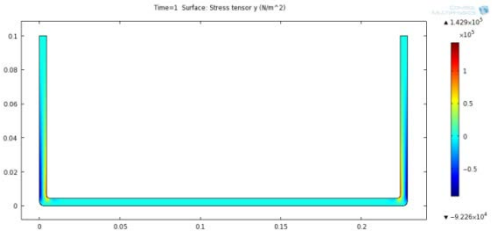

Fig. 11: Stress tensor (y-component)

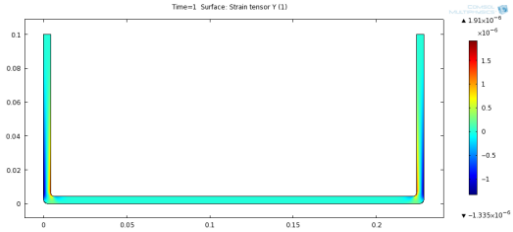

Fig. 12: Strain tensor (y-component)

The deformation load was obtained from the stress tensor plot (figure 13) as follows:

Area = 0.8749 m^2

Stress = 142900 Nm^{-2}

$$Stress = \frac{Force}{Area}$$

$$\therefore Force = Stress \times Area$$

$$= 142900 \times 0.8749$$
$$= 125023.21N$$
$$\approx 125KN$$

4.0Discussion

Figure 5 gives the value of the effective stress in the wall of the hollowware . The figure shows that stress is not uniformly distributed over the material body. The region of the maximum stress is at the inner corner of the pot as shown in figure 6. Within the wall, stress varies with a minimum at the center of the wall increasing towards the inner and outer sides of the hollowware (Figure 7). Stress variation down the wall does show that the value of stress increased from the top of the hollowware with a maximum at the base of the hollowware (Figure 8).

The positive and negative signs associated with values of strain tensor show the direction of the displacement of the particles of the pot during the deep drawing process of the blank. There were, therefore, some sort of compression and tension during deep drawing.
The value of deformation load was observed to be in conformity with industry value.

5.0 Conclusion

Finite Element Method (FEM) is a useful tool for stress analysis in deep drawing process. The most stressed part of a deep drawn hollowware is its base corner. The deformation load should be measured in this region.

References

[1]L.Herrmann, and G.Sachs, Untersuchungenüber das Tiefziehen.*Metallwirtschaft*13.40: 687-710. 1934.

[2]R.Hill, "*The mathematical theory of plasticity*", Oxford: Clarendon press.1950

[3]S.Y. Chung and H.W. Swift, "Cup drawing from a flat blank". *Proceedings of the institution of mechanical engineers* 165: 193-223. 1951.

.[4]A.S. Korhonen, "Drawing force in deep drawing of cylindrical cup with flat-nosed punch".*Journal of engineering for industry* 104: 29-37. 1982.

[5]D.M Woo, "Analysis of deep-drawing over a tractrix die".*Journal of Engineering Materials and Technology, Transactions of the ASME, 98 Ser H* 4: 337-341. 1976

[6]S. Louis, and W.Göppingen, *Metal forming handbook.* Ed. 1966.

[7]A.A. Pourkamali,M. Shahabizadeh and B.Babaee, " Finite Element Simulation of Multi-Stage Deep Drawing Processes & Comparison with Experimental Results" *World Academy of Science, Engineering and Technology* 61. 2012

[8]K. Siegert. and S.Wagner, Deep Drawing.*Training in aluminium application technologies (TALAT) Lecture 3704. 1994*

[9]H.H.Gharib, "Analysis of the Cup Drawing Process and Optimization of the Blank Holder Force".M.Sc. Dissertation, The American University in Cairo, Cairo, Egypt.2004.